



OPEN ACCESS

EDITED BY

Harold J. Schreier,
University of Maryland, United States

REVIEWED BY

Emma Berta Gutiérrez Cirlos,
National Autonomous University of Mexico,
Mexico
Vineet Kumar,
The University of Texas at Austin, United States

*CORRESPONDENCE

Karina Tuz
✉ ktuz@iit.edu

RECEIVED 12 August 2024

ACCEPTED 11 October 2024

PUBLISHED 06 November 2024

CITATION

González-Montalvo MA, Sorescu JM,
Baltes G, Juárez O and Tuz K (2024) The
respiratory chain of *Klebsiella aerogenes* in
urine-like conditions: critical roles of NDH-2
and *bd*-terminal oxidases.
Front. Microbiol. 15:1479714.
doi: 10.3389/fmicb.2024.1479714

COPYRIGHT

© 2024 González-Montalvo, Sorescu, Baltes,
Juárez and Tuz. This is an open-access article
distributed under the terms of the [Creative
Commons Attribution License \(CC BY\)](#). The
use, distribution or reproduction in other
forums is permitted, provided the original
author(s) and the copyright owner(s) are
credited and that the original publication in
this journal is cited, in accordance with
accepted academic practice. No use,
distribution or reproduction is permitted
which does not comply with these terms.

The respiratory chain of *Klebsiella aerogenes* in urine-like conditions: critical roles of NDH-2 and *bd*-terminal oxidases

Martín A. González-Montalvo, Jennifer M. Sorescu,
Gabriella Baltes, Oscar Juárez and Karina Tuz*

Department of Biological Sciences, Illinois Institute of Technology, Chicago, IL, United States

Klebsiella aerogenes is an opportunistic nosocomial bacterial pathogen that commonly causes urinary tract infections. Over the past decades, *K. aerogenes* strains have acquired resistance to common antibiotics that has led to the rise of multidrug-resistant and even pandrug-resistant strains. Infections produced by these strains are nearly impossible to treat, which makes *K. aerogenes* a global priority to develop new antibiotics and there is an urgent need to identify targets to treat infections against this pathogen. However, very little is known about the metabolism and metabolic adaptations of this bacterium in infection sites. In this work, we investigated the respiratory metabolism of *K. aerogenes* in conditions that resemble human urine, allowing us to identify novel targets for antibiotic development. Here we describe that, unlike other gram-negative pathogens, *K. aerogenes* utilizes the type-2 NADH dehydrogenase (NDH-2) as the main entry point for electrons in the respiratory chain in all growth conditions evaluated. Additionally, in urine-like media, the aerobic metabolism as a whole is upregulated, with significant increases in succinate and lactate dehydrogenase activity. Moreover, our data show that the *bd*-I type oxidoreductases are the main terminal oxidases of this microorganism. Our findings support an initial identification of NDH-2 and *bd*-I oxidase as attractive targets for the development of new drugs against *K. aerogenes* as they are not found in human hosts.

KEYWORDS

bacteria metabolism, *bd*-terminal oxidase, *Enterobacter aerogenes*, *Klebsiella aerogenes*, NDH-2, oxidase, urine

Introduction

Klebsiella aerogenes, formerly *Enterobacter aerogenes*, is a gram-negative, rod-shaped, motile, non-spore-forming bacterium (Grimont and Grimont, 2005). *K. aerogenes* is found in a plethora of niches, ranging from soil and water to the human and animal microbiota, where it is a commensal in the intestine (D'Alessandro et al., 2014; Davin-Regli and Pagés, 2015; Szczerba et al., 2020). *K. aerogenes* is also an opportunistic pathogen (Arpin et al., 1996; Davin-Regli and Pagés, 2015; Wesevich et al., 2020) that has caused several nosocomial outbreaks in the last few decades (Meyers et al., 1988; Allerberger et al., 1996; Arpin et al., 1996; Davin-Regli et al., 1996; Diene et al., 2013). This bacterium commonly produces respiratory infections, blood stream infections and urinary tract infections (UTIs) (Souza Lopes et al., 2016; Arpin et al., 2005; Arpin et al., 2003; Allerberger et al., 1996). Indeed, *K. aerogenes* is one of the most common causes of UTIs, besides uropathogenic *Escherichia coli* (Lodise et al., 2022). Complicated UTIs caused by *K. aerogenes* are often associated with resistance to commonly prescribed antibiotics, such

as nitrofurantoin and third-generation cephalosporins (Lodise et al., 2022). *K. aerogenes* is able to adapt quickly during antibiotic treatment, causing therapy failure that is often fatal (Beckwith and Jahre, 1980; Petit et al., 1990; Chow, 1991; Diene et al., 2013). The number of cases caused by extended-spectrum beta-lactamase (ESBL)-producing *Enterobacterales*, including *K. aerogenes*, have alarmingly increased in the last 20 years, and the CDC has classified ESBL-producing *Enterobacterales* as serious threats that require prompt action (Centers for Disease Control and Prevention, 2019). Carbapenems have been widely used as antibiotic therapy against ESBL-producing pathogens, which quickly led to the emergence and propagation of carbapenem-resistant *Enterobacterales* (CRE), further reducing treatment options. In the US, *K. aerogenes* is one of the most common CRE (Karlsson et al., 2022) and the CDC has recently identified CRE microorganisms as public health threats that require urgent action (Centers for Disease Control and Prevention, 2019). In addition to beta-lactams and carbapenems, resistance to third-generation cephalosporins has been observed in a high percentage of isolated CRE *K. aerogenes* strains (Gashe et al., 2018), which produce nearly untreatable infections. The WHO (World Health Organization, 2017) has recognized *K. aerogenes* as a pathogen for which antimicrobial development is critically needed due to multidrug-resistance and its role in nosocomial infections (Mulani et al., 2019), ultimately leading to high risk of mortality and increased health care costs (Founou et al., 2017).

It is evident that new targets are urgently needed to treat infections caused by this pathogen. Targeting the molecular mechanisms used by the pathogen to survive and adapt to the host internal environment represents a novel alternative to produce antibiotics. However, little is known about the metabolism and physiology of *K. aerogenes*, or its metabolic adaptations in pathologically relevant conditions. Genomic analyses indicate that *K. aerogenes* codes for around 121 genes related to respiration or metabolism (Mann et al., 2021). However, the actual number and type of enzymes used in different conditions are almost completely unknown. Our group has previously described that respiratory enzymes in other bacteria, such as *Pseudomonas aeruginosa* (Liang et al., 2020) and *Chlamydia trachomatis* (Liang et al., 2018), are promising new targets for drug development, as these enzymes are not found in the human genome and their structural motifs are absent in human enzymes. Understanding the respiratory strategy of *K. aerogenes*, particularly in host-like conditions, may allow us to carry out drug design on specific targets that are essential for the growth and infectious process of this microorganism.

The aim of this work is to understand the respiratory pathway of *K. aerogenes* in conditions mimicking human urine. Our results show that this pathogen uses the type D₂ NDH-2 dehydrogenase as the main NADH dehydrogenase and as the main entry point of electrons into the respiratory chain, and that the *bd-I* type terminal oxidase plays a major role in the electron transport chain. The data also show that this microorganism adapts its metabolism in urine-like conditions, increasing the expression of succinate dehydrogenase (SDH) and lactate dehydrogenase (LldD). These results provide essential information to understand the metabolic strategies used by this pathogen in colonization of the urinary tract and to propose alternatives for antibiotic treatment through the identification of targets for drug development.

Materials and methods

In silico screening of enzymes involved in respiration

Respiratory enzymes were identified in the *K. aerogenes* ATCC® 35029 genome using a BLAST search approach. Sequences used as query were downloaded from Uniprot (Supplementary Table S1) and used in a local tBLASTn. Results were manually curated to eliminate false positives.

Growth analysis

Klebsiella aerogenes ATCC 35029 growth behavior was assessed in LB and modified artificial urine media (mAUM), which was recently developed by our group (Liang et al., 2020). Growth curves were performed in 500 mL baffled flasks. Bacterial cultures were incubated at 37°C with shaking at 250 RPM. Samples were collected regularly, diluted and plated on LB plates; colony counts were determined after overnight incubation at 37°C. Experiments were performed at least three times on different days. To calculate the growth rate, maximum growth and lag phase length, growth curves were fitted to logistic functions as described previously (Liang et al., 2020).

Isolation of *Klebsiella aerogenes* membranes

Klebsiella aerogenes ATCC 35029 cells were grown in either LB or mAUM. Bacterial cells were harvested by centrifugation (10,000 × g for 30 min at 4°C) during mid-log phase. Bacterial pellets were washed twice with KHE buffer (150 mM KCl, 20 mM HEPES, 1 mM EDTA, pH 7.5) and stored at −80°C. Frozen pellets were thawed on ice and homogenized in KHE buffer with 10 μg/mL DNAase I, 5 mM MgCl₂ and 1 mM PMSF. Cells were lysed at 16,000 PSI using an Emulsiflex-C5 homogenizer. The cell lysate was centrifuged at 1,500 × g for 1 h to remove unbroken bacteria. Then the supernatant was spun at 48,000 × g for 1 h to remove cellular debris. Afterwards, the supernatant was centrifuged at 100,000 × g for 4 h to obtain the membrane pellet. The pellet was washed with KHE buffer and centrifuged at 100,000 × g for 1 h. The membrane pellet was resuspended in KHE buffer, aliquoted and stored at −80°C until further use.

Oxygen consumption measurements

Oxygen consumption rates (OCR) of isolated *K. aerogenes* membranes were assessed using a YSI 5300 Clark-type electrode fitted to a 1.6 mL custom-made glass chamber. Oximetric analyses were performed using 0.1 mg/mL of protein in the presence of specific substrates and inhibitors for all respiratory complexes. NADH oxidase activity was measured using 200 μM NADH or 200 μM deamino-NADH with or without 1 μM rotenone. The activity of succinate dehydrogenase was measured using 20 mM succinate. For non-canonical ubiquinol-dependent respiratory enzymes, 10 mM lactate was used to measure the activity of lactate

dehydrogenases, 10 mM D/L-malate for malate dehydrogenases, 10 mM D-glucose for glucose oxidases and 0.3% ethanol for alcohol dehydrogenases. Cytochrome *c* oxidase activity was measured using 100 μ M TMPD (N,N,N',N'-tetramethyl-p-phenylenediamine) and 5 mM ascorbic acid. Ubiquinol oxidase activity was evaluated using 50 μ M of either ubiquinone-1 or menaquinone-2 reduced in the presence of DTT, as previously reported (Liang et al., 2020).

KCN titration

The participation of terminal oxidases in the respiratory metabolism in *K. aerogenes* membranes was estimated carrying out a titration with KCN (0.1–10 mM). The titration curve was analyzed as previously described by our group (Liang et al., 2020), fitting the data to a two-component equation, assuming that the concentration of substrates is near saturation ($[S]/K_m > 10$).

Blue native gel electrophoresis

Membrane samples were washed and resuspended in Buffer M (50 mM Bis-Tris, 500 mM aminocaproic acid, pH 7.0). Membranes were solubilized using Triton X-100 at a protein: detergent ratio of 1:2. The samples were incubated on ice for 40 min and centrifuged at 120,000 $\times g$ for 40 min. Solubilized membranes were mixed with Cathode Buffer I (50 mM Tricine, 15 mM Bis-Tris, 0.02% Coomassie Brilliant Blue G-250, pH 7.0) at a 5:1 ratio and applied to a 4–16% gradient native polyacrylamide gel, as described previously (Liang et al., 2020). For NADH activity, gels were incubated in NADH Reaction Buffer (100 mM Tris-HCl, 140 μ M NBT, pH 7.4) for 1 h.

Proteomic analysis

LB or mAUM membranes were solubilized in 1% SDS and centrifuged at 13,000 $\times g$ to remove non-solubilized debris. Protein preparation and analysis was performed by The Mass Spectrometry Core of the Research Resources Center of University of Illinois at Chicago. 50 μ g of protein per sample were filtered using 10K NMWL centrifugal filter units. Proteins were reduced by incubation in 20 mM dithiothreitol for 30 min and were alkylated with 50 mM iodoacetamide for 20 min in the absence of light. Samples were washed three times using buffer containing 8 M urea and 0.1 M ammonium bicarbonate. Afterwards, washed samples were equilibrated with 0.1 M ammonium bicarbonate and transferred to a buffer containing 0.1 M ammonium bicarbonate and trypsin at an enzyme: protein ratio of 1:20. The digestion was incubated at 37°C overnight. Peptides were recovered by centrifugation at 14,000 $\times g$ for 20 min and eluted twice with 50 mM ammonium bicarbonate with an additional elution using 0.5 M NaCl. Finally, samples were desalted with an Oasis Prime HLB and then dried. Digested samples were labeled using TMT 6plex isobaric Label Reagent Set (ThermoFisher, Waltham, MA, USA) following manufacturer's instructions. Samples were combined, dried and desalted using a primed HLB 96 well plate. Off-line high-HP reverse phase liquid chromatography was performed to obtain fractions which were concatenated in 6 pools. Pooled fractions were dried and resuspended in 5% acetonitrile and 0.1% formic acid buffer for LC-MS

analysis. Mass spectrometry data were searched against the Uniprot database of *K. aerogenes* proteins using Mascot Engine (2.6.0) with a parent mass tolerance of 10 ppm, a constant modification on cysteine alkylation, variable modification on methionine oxidation, deamination of asparagine and glutamine, and TMT purity correction. Results were analyzed in Scaffold Q+S Software v 5.0.0 (Proteome software, Portland, OR, USA) using filtering criteria of 1 minimum peptide count and a false discovery rate of 1%.

Results

Klebsiella aerogenes growth in urine-like medium

In this work, we characterized the growth of *K. aerogenes* in media that mimics human urine. For this purpose, we employed the previously described mAUM, developed by our group, which offers more stability and reliability compared to other urine-like media (Liang et al., 2020). There is no information regarding the growth behavior of *K. aerogenes* in standard laboratory media or physiologically relevant conditions, for this reason the results obtained in urine-like media were compared to the enriched laboratory media, LB broth (Figure 1). This helped us to understand the general metabolic pathways used by this pathogen and the adaptations to urine-like media. This organism was able to grow in both enriched and urine-like media, which in the constant agitation conditions used remained 80–85% oxygen saturated (measured with a Clark-type oxygen electrode, as described below). *K. aerogenes* showed typical sigmoidal growth in both media analyzed (Figures 1A,B). We observed that media composition influenced growth behavior, with higher bacterial counts in LB media (CFU/mL) than in mAUM (Figure 1C). In contrast to growth in enriched media, *K. aerogenes* displayed a slower growth rate and lower bacterial density in mAUM (Figure 1D), but no difference in the lag phase (Figure 1E), suggesting that this bacterium is able to quickly adapt to growth using components present in human urine. These results indicate that *K. aerogenes* carries the metabolic machinery that allows its adaptation during growth in urine and likely during urinary tract infections.

Klebsiella aerogenes respiratory genes

We identified and classified the genes involved in respiratory metabolism in the *K. aerogenes* genome from the NCBI repository, using different query sequences of each known membrane protein involved in aerobic respiration. Our search shows that the *K. aerogenes* genome contains genes that code for three NADH: ubiquinone oxidoreductases: NDH-1 (complex I-type), NDH-2 (two class D₂ and one class C enzymes) and NQR (Figure 2). NDH-1 is a proton-pumping dehydrogenase, composed of 13–14 subunits with one FMN and multiple Fe-S centers (Brandt, 2006). NQR is a six subunit, six cofactor (Juárez et al., 2008; Juárez and Barquera, 2012; Reyes-Prieto et al., 2014) respiratory enzyme that pumps sodium (Bogachev et al., 1997; Barquera et al., 2002), and at least in one case protons (Raba et al., 2018). NDH-2 is a single subunit and single cofactor dehydrogenase that does not pump ions and does not contribute to cell energetics (Ito et al., 2020). Other dehydrogenases

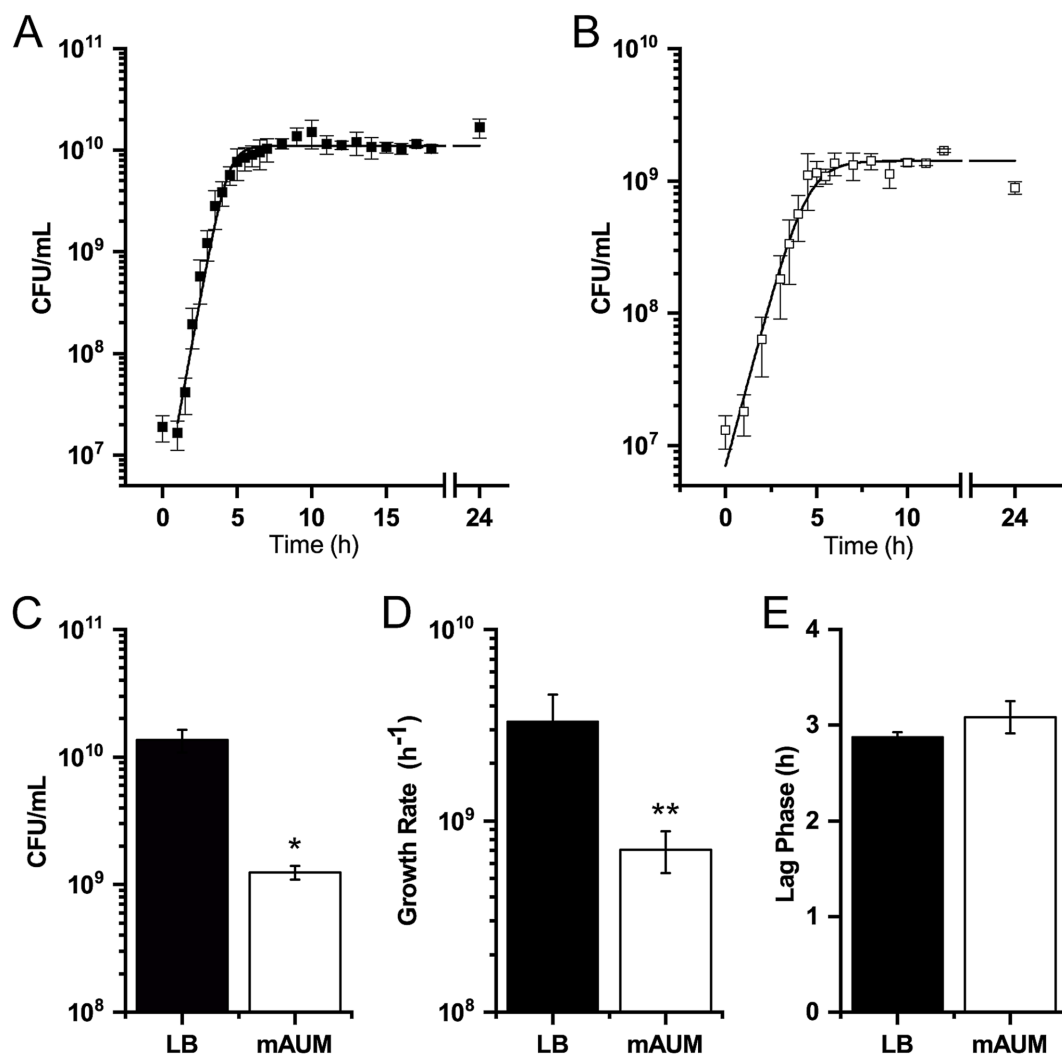


FIGURE 1

K. aerogenes growth in LB and mAUM. (A) Growth curve in LB broth. (B) Growth curve in mAUM. (C) Maximum growth. (D) Growth rate. (E) Duration of lag phase. Black bars represent data from LB and white bars indicate data from mAUM. Data are expressed as the mean \pm SD, $n = 3$. The asterisk indicates significance mAUM vs. LB (* $p < 0.05$, ** $p = 0.001$) determined by t -test analysis.

found in the genome are succinate dehydrogenase (SDH), three membrane-bound NAD-independent lactate: quinone oxidoreductases (LldD, DLD and LdhA) and two membrane-bound malate: quinone oxidoreductases (MQO1 and MQO2) (Figure 2). Moreover, we determined that this bacterium carries the genes coding for one cytochrome bo_3 terminal oxidase and four bd -type terminal oxidases. For the bd -type oxidases, two operons belong to the bd -I type and two to the bd -II type terminal oxidases. Furthermore, we found the genes involved in the biosynthesis of ubiquinone and the partial biosynthetic pathway of menaquinone, with the absence of MenA and MenG, which indicate that this quinone is not biosynthesized by *K. aerogenes*. This is in accordance with previous reports, which show that ubiquinone-8 is the sole quinone present in *K. aerogenes* under aerobic and anaerobic conditions (Knook and Planta, 1971, 1973). Finally, *K. aerogenes* encodes the machinery for biosynthesis of cytochrome c . However, it does not seem to have a role in aerobic respiration, as the bc_1 complex and cytochrome c oxidases are not found in the genome.

Klebsiella aerogenes metabolic repertoire is more active during growth in urine-like conditions

To identify the metabolic adaptations that *K. aerogenes* uses to grow in mAUM, we analyzed oxygen consumption rates in membranes using substrates of different enzymes involved in respiration. Our results show that oxygen consumption activity is higher in membranes obtained from cells grown in mAUM compared to LB (Figure 3), suggesting that the respiratory chain plays a major role in the adaptation to urine and likely in UTIs. In mAUM membranes, succinate dehydrogenase and lactate dehydrogenase activities showed a 2.5- and 4.4-fold increase, respectively, suggesting that *K. aerogenes* adapts its metabolism and uses the substrates present in urine to grow efficiently during UTIs. Although there were significant differences in the growth parameters, we found no difference in the NADH dehydrogenase or malate dehydrogenase activities in both conditions. Glucose

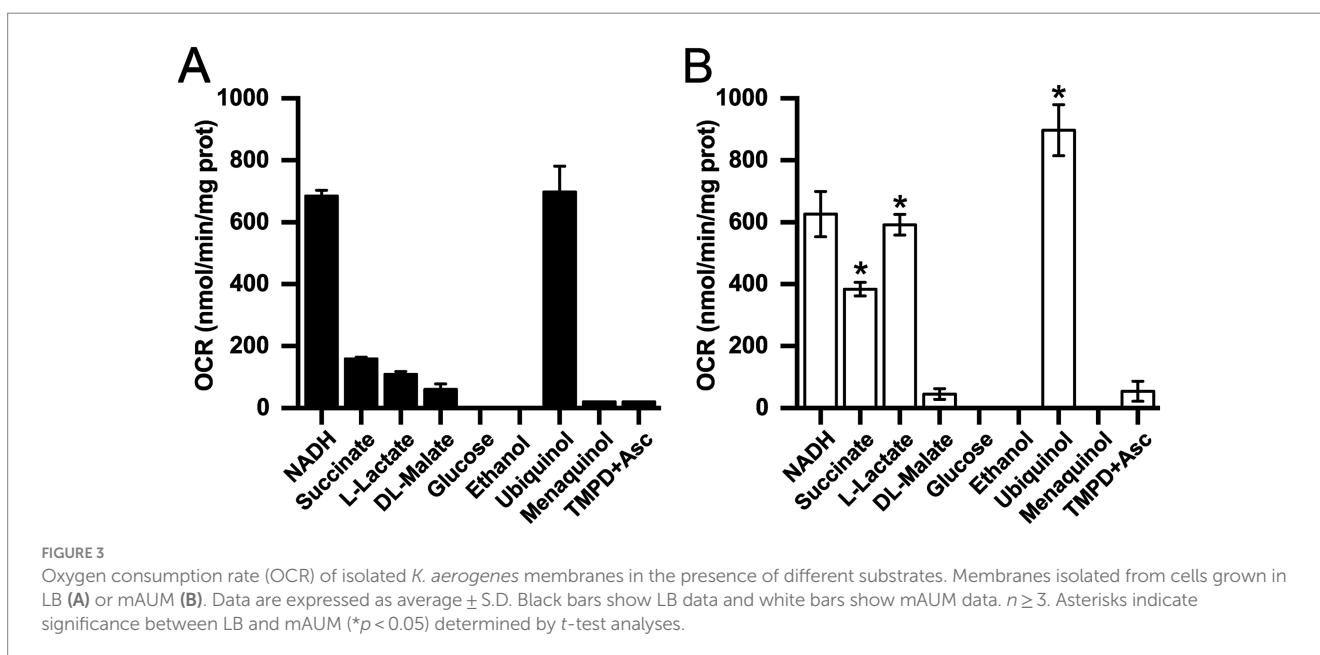
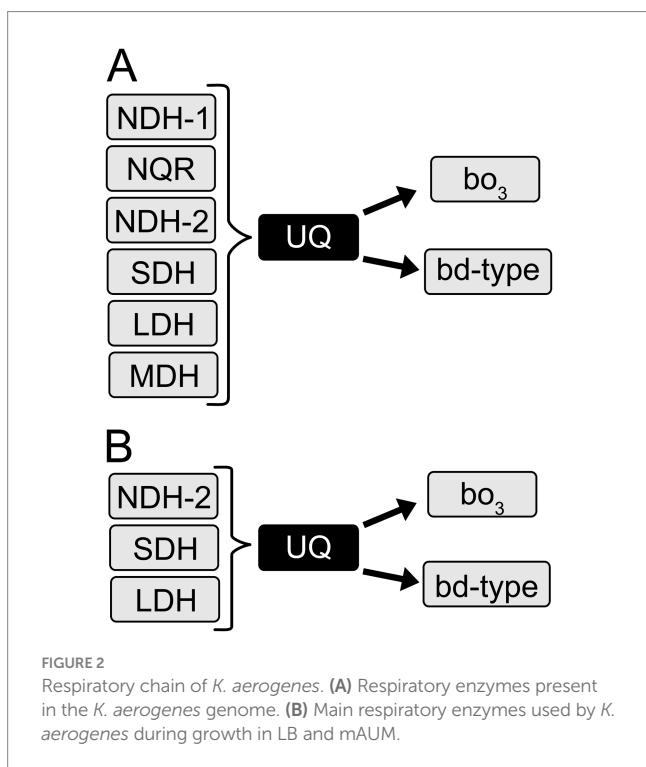
oxidase and ethanol dehydrogenase activities were negligible, indicating that these substrates are not used by the electron transport chain.

In addition to the dehydrogenases, we also studied the quinone preference of *K. aerogenes* respiratory machinery using ubiquinol-1 and menaquinol-2 as substrates for the terminal oxidases. Our results show that the terminal oxidases of cells grown aerobically, preferentially use ubiquinol in both mAUM and LB media. While LB membranes were able to use menaquinol at low rates, no menaquinol

oxidase activity was detected in mAUM (Figure 3). Additionally, we found that the activity with TMPD and ascorbate is negligible, indicating that this microorganism does not use cytochrome *c* oxidases, confirming the results obtained from the genome analysis.

NDH-2 as the main NADH dehydrogenase in *Klebsiella aerogenes*

Although NDH-1, NDH-2 and NQR catalyze the same chemical reaction, they can be differentiated by substrate specificity and inhibitor selectivity. NDH-1-type dehydrogenases employ NADH and deamino-NADH as substrates, and are susceptible to inhibition by rotenone (Yagi, 1991; Zickermann et al., 2000; Melo et al., 2004). NQR can also use NADH and deamino-NADH as substrates, but it is insensitive to rotenone (Zhou et al., 1999; Hreha et al., 2021). NDH-2 is insensitive to rotenone and can only use NADH as substrate (Yagi, 1991; Melo et al., 2004; Hreha et al., 2021). As shown in Figure 4A, the deamino-NADH oxidase activity in membranes is <10% in LB and <20% in mAUM compared to the NADH oxidase activity, indicating that NDH-2 is the main NADH dehydrogenase in this organism (Figure 4B). Rotenone does not significantly inhibit the deamino-NADH independent activity and thus we can assign NQR as the second most important dehydrogenase in LB. In mAUM, the NDH-1 activity is higher compared to the activity of NQR. To corroborate the activity data, we conducted Blue Native Gel electrophoresis analysis of the respiratory complexes in membranes solubilized with 1% Triton X-100. The three NADH dehydrogenases can also be differentiated by their electrophoretic mobility in native gels, as NDH-1, NQR and NDH-2 have estimated molecular weights of 550 kDa (Yip et al., 2011), 200 kDa (Juárez and Barquera, 2012) and 47 kDa (Yagi, 1991), respectively. As shown in Figure 4C, the samples ran in BN-PAGE contain a single band with NADH dehydrogenase activity of approximately 132 kDa. This band is too small to correspond to NDH-1 or NQR and likely corresponds to an NDH-2 dimer. The



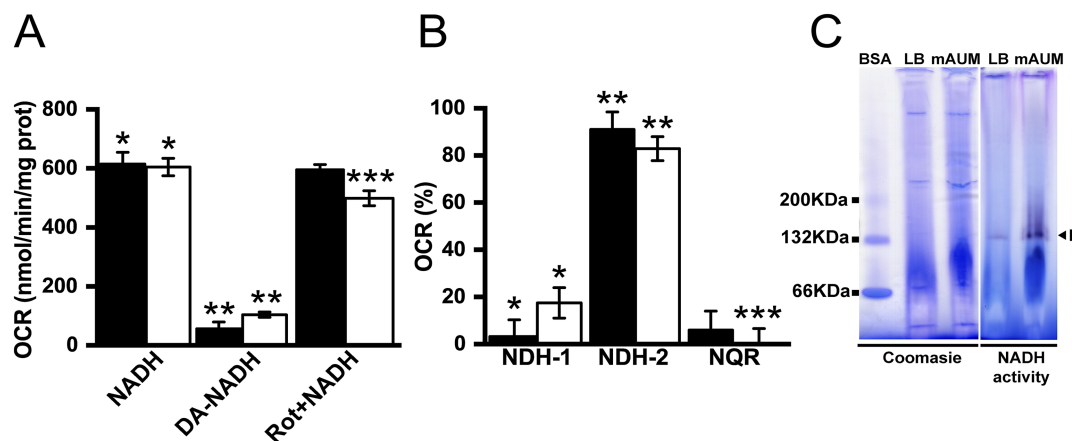


FIGURE 4

NADH dehydrogenases in *K. aerogenes* membranes. (A) Oxygen consumption rate using NADH, deamino-NADH (DA-NADH) and rotenone (Rot). (B) Participation of NADH dehydrogenases in oxygen consumption rates. (C) NADH dehydrogenase activity observed in blue native gel. Label I indicates a band of approximately 132 KDa (arrow head). BSA in its different oligomeric states is used as weight marker. Black bars correspond to data obtained from LB and white bars from mAUM. Data are expressed as average \pm SD. *t*-test statistical analyses were performed for panels (A,B) ($p < 0.05$), asterisks correspond to comparison between groups: (A) *NADH vs. DA-NADH; **DA-NADH vs. Rotetone; ***NADH vs. Rotenone. (B) *NDH-1 vs. NDH-2; **NDH-2 vs. NQR; ***NDH-1 vs. NQR.

presence of a dimeric NDH-2 has been previously reported in other organisms, including *Caldalkalibacillus therrmarum* (Feng et al., 2012; Heikal et al., 2014; Nakatani et al., 2017).

As described above, *K. aerogenes* carries three NDH-2 genes, two class D₂ and one class C. To identify the main NDH-2 enzyme involved in electron transfer, we carried out proteomic analysis of membranes obtained in LB and mAUM. As shown in Figure 5A, mass spectrometry identified peptides belonging exclusively for NDH-2 D₂-1, indicating that this is the NDH-2 responsible for the NADH dehydrogenase activity and most of the NADH-dependent respiration in this microorganism.

Bd-type oxidases are the main terminal oxidases in *Klebsiella aerogenes*

To elucidate the contribution of terminal oxidases to the respiratory metabolism in *K. aerogenes*, a KCN titration of the respiratory activity was carried out. Testing the cyanide susceptibility of the respiratory activity is a useful method to estimate the participation of the terminal oxidases, as the reported K_{iapp} for KCN of the terminal oxidases differs by more than one order of magnitude. For instance, the K_{iapp} of bo_3 oxidases is significantly lower than *bd* oxidases, typically ranging from 10 to 40 μ M (Mogi et al., 2009; Weiss et al., 2010; Melin et al., 2013; Liang et al., 2020), although significant variability has been observed (see below), while the K_{iapp} of *bd*-oxidases ranges from 1 to 30 mM (Matsushita et al., 1983; Forte et al., 2017). The titration data obtained for both types of membranes was best fitted to a two-component inhibition model (Figure 6). The first component, representing 27–32% of the activity in both types of membranes, has a K_{iapp} of $0.2 \pm 0.1 \mu$ M in LB and $0.3 \pm 0.05 \mu$ M in mAUM membranes, likely corresponding to bo_3 -type oxidases. The second component has a K_{iapp} of $106 \pm 14 \mu$ M in LB and $123 \pm 2 \mu$ M in mAUM, accounting for 76–81% of the respiratory activity and likely corresponding to *bd*-type oxidases. Thus, our results indicate that

bd-oxidases are the main terminal oxidases in *K. aerogenes*, and for this reason, we decided to carry out proteomic analysis to identify the main enzyme.

As described above, *K. aerogenes* carries two *bd*-I (*cydABX*-1 and *cydABX*-2) and two *bd*-II oxidase operons (*appCBX*-1 and *appCBX*-2), as well as one bo_3 operon (*cyoABCDE*). In order to identify the specific enzymes expressed by this pathogen in mAUM and LB media, we performed proteomic analysis of isolated membranes from bacteria grown in the two different media (Figure 5). Proteomic analysis demonstrates the presence of subunits CyoA and CyoB of the bo_3 oxidase, as the next peptides were identified for CyoA (accession number A0A0F1LA05): GQIGLEQR, YSPNWSHSNK, VTSNSVMNSFFIPR, ATFDQWVAK, QSPNSMDSMAAFDK and VAVPSENNK, and for CyoB (accession number A0A44LCJ9): APGMTMFK, AFGFTLNETWGK, DLTGDPWGGR, TLEWATSSPPPFYNFVAVPNVHER, QPAHYEEIHMPK, SFDEDVDYYVPVAEVEK and LENQHDFEINK. Our data also show that of the four *bd*-type enzymes, only the *bd*-I encoded in the *cydABX*-1 operon was expressed in these membranes (Figure 5B). This operon is located in a genetic locus similar to the *E. coli cydABX* operon, which is differentiated from other *cydABX* operons by the presence of the *ybgE* and *ybgC* genes, flanked by *sdhCDAB*, *sucABCD* and *tolQRAB* operons (Muller and Webster, 1997). In *E. coli*, *cydABX* codes for the main terminal oxidase in this microorganism during the stationary phase and under microaerophilic conditions (Tseng et al., 1996; Grund et al., 2021).

Proteomic analysis of *Klebsiella aerogenes* membrane associated transporters and respiratory enzymes

A proteomic analysis was performed to propose the metabolic machinery employed by *K. aerogenes* during growth in urine-like conditions by comparing the content of respiratory enzymes and

A

Id. Peptides
 Ndh-2 D2-1 1 MTTPLKRIIVVGGGAGGLELATQLGRKLGRRNK - -AKITLVDRNHSHLWPKLLHEVATGSLDEGVDALSYLAHARNHGQFQLGSSV 85
 Ndh-2 D2-2 1 MTTPLKEIIVVGGGAGGLELATQLGRKLGRRNK - -ANNITLVDRSQSHLWPKLLHEVATGSLDEGVDALSFLAHASKHHFSFQHGSVI 85
 Ndh-2 C 1 - - -MRKQILIVGAGFAGMWAALSAARLAENKQQQAIDITVIAQPQELRVRPRFYESDVPSSLVAPLQPL - - - -FDATGIRFLRGSVS 79

Id. Peptides
 Ndh-2 D2-1 86 DINREGKTI LAELRNEK**GELLVAER**KLPYDTLVMLGSTSNDFNTPGVK**ENCIFLDNPHQAR**RFHQEMLNLF**YSANLGGANGK**VN 172
 Ndh-2 D2-2 86 DIDRQNKTI I AALRDEQGEVLVPERKLCWDTLVMLGSTSNDFNTPGVK**ENCIFLDNPHQAR**RFHQEMLNLF**YSANLGGANGK**VN 172
 Ndh-2 C 80 QIHPADKTVTWTGSGNES - - - - -HTQNWDRVLVLSGSHVNRAMVTGAAQHAFDLDQLESATTLENHLIALAQR - - - -PQSDARNT 155

Id. Peptides
 Ndh-2 D2-1 173 IAIVGGGATGVLSAELHNAVQLHSYGYK**GLTNEALNVTLVEAGERILPALPPR**ISGAHNELTKLGVRLTQTMVTSADVNGLHT 259
 Ndh-2 D2-2 173 IAIVGGGATGVLSAELHNAVQLRSYGYK**GLTNEALNVTLVEAGERILPALPPR**ISGAHNELTKLGVRLTQTMVTSADVNGLHT 259
 Ndh-2 C 156 VVCGGGFTGIEAMELPTKLRAIFG - - - - -SNAKTRVVVVERGPPGSRYSALREVIVQASKELGVEVLVNAEAVSVAAGVKL 236

Id. Peptides
 Ndh-2 D2-1 260 KDGQFIDADLMVWAAGIKAPDFMK**EIGGLETRINQLVVEPTLQTRDPIYAI**IGDCASCARPEGGFVPPR**AQAAHQMATCALNNI** 345
 Ndh-2 D2-2 260 KDGQFIEASLIVWAAGIKAPDFMK**EIGGLETRINQLVVEPTLQTRDPIYAI**IGDCASCARPEGGFVPPR**AQAAHQMATCALNNI** 345
 Ndh-2 C 237 KDGQRIDSQTVIWTVGQANNLTAQIDAPRD-RQGRHLVNAELQVMGYDDIYATGDVYAAATDDKGNHALMTCQHAILLGKFAGNNA 322

Id. Peptides
 Ndh-2 D2-1 346 LAQMKGKALKPYVYKDHGSLVLSNSTYVGSMLGNLMRGSMMVEGR IARFVYISLYRMHQIALHGFKTGLMMLVGRINRIRPRLK 432
 Ndh-2 D2-2 346 IARMKGHKLKSFYSYDRGSLVLSGYTTFGSIIMGHLP IGPMMVEGR IARMVYDLYRMHQVTLHGFKTGLMMLSGGINRIRPRLK 432
 Ndh-2 C 323 AAGLLG - -VAPLHYR-QETYVTCTLDLGAWAVYTEGWDQVVKLTREEAKVKVSVISELIYPPKADKTSAFEMADP - - - -LAPFV - 400

Id. Peptides
 Ndh-2 D2-1 433 LH 434
 Ndh-2 D2-2 433 LH 434
 Ndh-2 C - -

B

Id. Peptides
 CydA-1 1 - -MLDIVELSRQLFALTAMYHFLVPLTLGMAFLLAIMETVYVLSGKQIYKDMTKFWGKLFGINFALGVATGLTMEFQFGTNSWY 83
 CydA-2 1 MAEFDAFHLARIQFAFTISFHIIFPALITGLASLVVLEGMWLKTRRLWLRQLYHFWLNI FAI NFGMGVVSGLVMAYQFGTNSWG 85
 AppC-1 1 MFGLDFAHLARIQFAFTVSFHIIFPAITIGLASYLAVLEGLWLTKNPVWRSLYHFWSKI FAVNFGMGVVSGLVMAYQFGTNSWG 85
 AppC-2 1 MFGLDFAFLYARIQFAFTVSFHIIFPAITIGLASYLAVLEGLWLTKEITYRQLYHFWSKI FAVNFGMGVVSGLVMAYQFGTNSWG 85

Id. Peptides
 CydA-1 84 YSHYVGDIFGAPLAI EGLMAFFLESTFVGLFFFGWDRLGKQVHMAVTVLVALGNSLSALWILVANGWMQNP IASDFNFETMRMEM 168
 CydA-2 86 FSQFAGSI TGPLLTYEVLTAFFLEAGFLGVMLFGWNRVGPGLHFFSTCMVAIGTLASTFWILASNSWMQTPQG - -FHI EQGQV I P 168
 AppC-1 86 FSQFAGSI TGPLLTYEVLTAFFLEAGFLGVMLFGWNRVGPGLHFFSTCMVAIGTLASTFWILASNSWMQTPQG - -FHI EQGQV I P 168
 AppC-2 86 FSQFAGSI TGPLLTYEVLTAFFLEAGFLGVMLFGWNRVGRGLHFFSTCMVAIGTLASTFWILASNSWMHTPQG - -YI IENGIVVP 168

Id. Peptides
 CydA-1 169 VSFSELVLPVAVQKVFVHTVASGYVTGAMFILAISWYMLKGRDFAFAKRSFAIAASFGMAA ILSVIVLGDSEGYEMGDVQKTKL 253
 CydA-2 169 DSWLAIIFNPSFPWRLLHMSIAAFLSTALFVGASAAWHLRDNTPAIRTFMSMALWMLIVAPIQAVVGDMMHGLNLTLLKHQPAKI 253
 AppC-1 169 VDWFAVIFNPSFPYRLLFHMSSAAFLSSALFVGASAAWHLRGNHTPAIRAMFSMALWMLTLLVAPIQAMIGDMHGLNLTLLKHQPAKI 253
 AppC-2 169 VDWLKVVFNPSFPYRLLHMSIAAFLSAFFVGASAAWHLKGNTPAIRKMFMSMALWMLIVAPIQAMIGDAHGLNLTLLKHQPAKI 253

Id. Peptides
 CydA-1 254 AAIEAEWETQP-APAAFTLFGIPDQEAQTNHFSIQIPYALGIIATRSV**VDKPVIGLKDLMQAHEER**RY**AYALLEQL** 314
 CydA-2 254 AAIEGHWENKPGEATPLLLFGLPDMAEERTRYPLAIPALGSLILTHSRSAQVPALKDFPAN - - - - - 314
 AppC-1 254 AAIEGHWENPPGEPTPLLLFGWPDQERTRYGLEIPALGSLILTHSLDKQVPALKEFAPE - - - - - 314
 AppC-2 254 AAIEGHWENKPGEATPLVLFGLPDMDEERTKYKIEVYPLGSIILTHSLDKQVPALKSFPKE - - - - - 314

Id. Peptides
 CydA-1 338 QAVRDRFNDVKK**DLGYGLLLKRYTPNVADATEEQIAK****DSIPSVAPLYFAFR**IMVACGVLMLLIGASFWTVIRNRI GEKKWL 422
 CydA-2 315 - - - - -**DRPNSTIVFWSFRFMVAGFLMIALGVI**GWYLRHRKRLCDSRPF 358
 AppC-1 315 - - - - -**DRPNSTIVFWSFRFMAGLGLMLILLGVI**ALWLYRQRRLYTSKPF 358
 AppC-2 315 - - - - -**DRPNSTIIFWSFRVMAGLGLMLVLLGVVSAWLRWRGRRLYTSKPF** 358

Id. Peptides
 CydA-1 423 LRAAFFGLPLPWI AVEAGWFAEYGRQPWAIGEVLPTAVANSSLTAGDLIFSMILLICGLYTLFLVAELFLMFKFARKGPSLKTG 507
 CydA-2 359 LWFALAMGPVGLLTI LAGWITTEVGRQPWVVYGLLRTRDAVSAHSTLQMSVSLTAFVVVYFAVFGVGYLYLIRLLKLGPPQ - ESE 442
 AppC-1 359 LRFALWMPGSLIAI LAGWVTEVGRQPWVVYGIQRTSEAVSAHGLDHMTISLLAFI AVYSSVFGVGYSMYLRIRLIRKGPQ - - - - E 439
 AppC-2 359 LRFALLMGPSGLVALLAGWFTTEIGRQPWVVYGRTRDAVSAHGLDHMSLSELLAFIVVYASVFGVGYVYLIRLIRKGPESAHTP 443

Id. Peptides
 CydA-1 508 RY**HFQSSAAIQSAR** - - - - - 465
 CydA-2 443 LALNSSGTPARPLSAPDKLPSEEK - - - - - 469
 AppC-1 440 QTPVPSGTPARPLSAAIDGFGHKESR 522
 AppC-2 444 EDPTQNTPARPLSAVREPMNTSGRK 467

FIGURE 5
 Sequence analysis of peptides. (A) Alignment of the *K. aerogenes* NDH-2 dehydrogenases and the peptides identified by proteomic analysis. (B) Alignment of subunit I of *K. aerogenes* bd-type terminal oxidases. Black boxes indicate the sequence of the peptides found in proteomic analysis. Alignment of amino acid sequences was performed on ClustalX2.

membrane associated transporters of membranes of cells grown in LB and mAUM. As indicated above, NDH-2 is the main NADH-dehydrogenase in both conditions (Figure 4). Although oximetry data did not show a significant change in the overall NADH dehydrogenase activity in mid-log growth among both conditions,

the content of the different enzymes changed in mAUM when compared to LB as determined by proteomic analysis: the NDH-2 (D2-1 isoform) showed a small decrease (0.8-fold change ratio), a significant increase (1.5 fold-change on average) of NDH-1 was observed as determined for Nuo proteins, and we also observed a

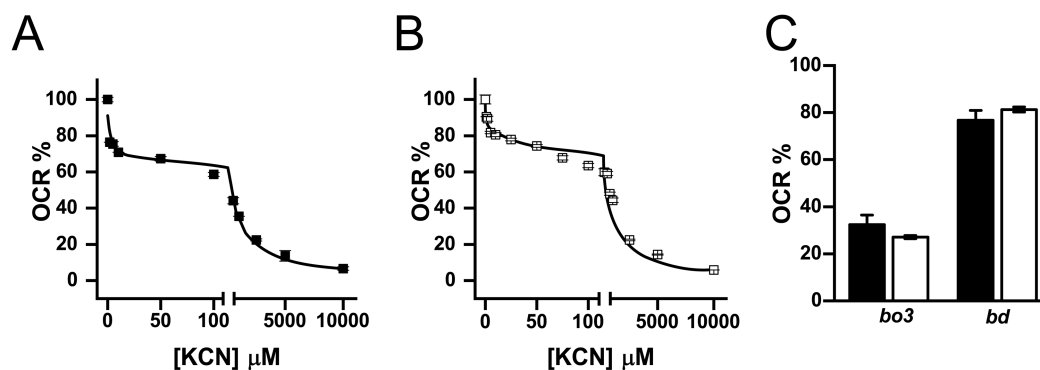


FIGURE 6

Contribution of terminal oxidases to the respiratory activity of isolated *K. aerogenes* membranes. Oxygen consumption rate was measured under increasing concentrations of KCN. KCN titration of LB (A) and mAUM (B) membranes using a two-component formula (see material and methods). (C) Relative contribution of *bo3* and *bd*-type oxidases to the respiratory activity of LB (black bars) or mAUM (white bars). Data expressed as average \pm S.D. $n \geq 3$.

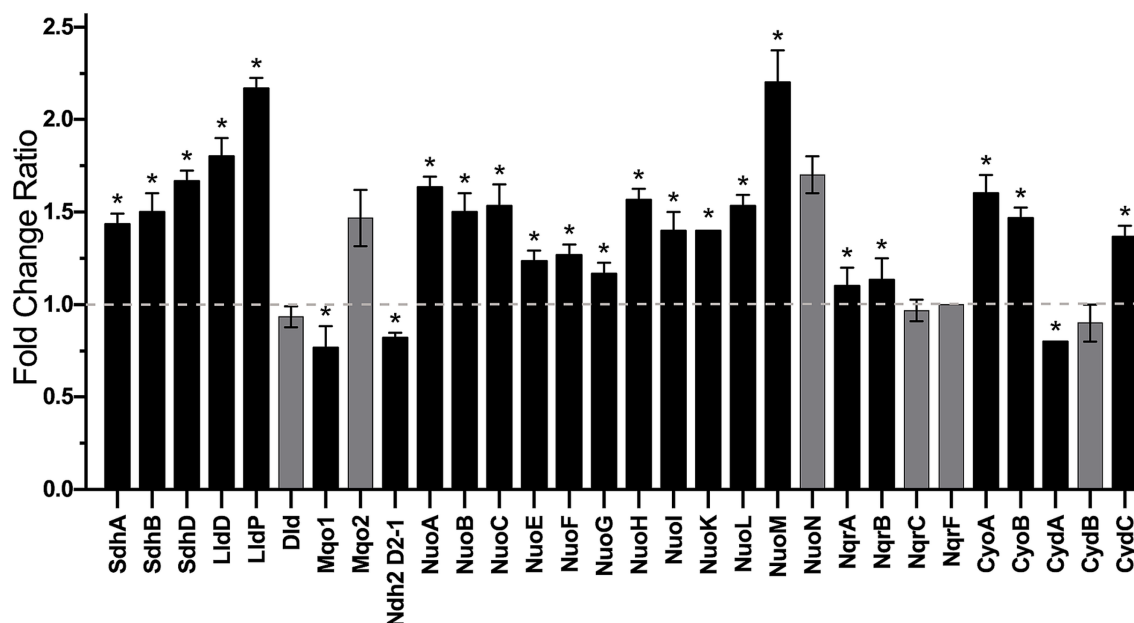


FIGURE 7

Proteomic data of main NADH-dehydrogenases, NADH-independent ubiquinone-dependent dehydrogenases and terminal oxidases. Fold change ratio of mAUM data vs. LB data is shown. Dashed line indicates no change. Data represent average \pm S.D., $n = 3$. Asterisks denote significance ($p = 0.01$) as determined by *t*-test. Non-significant change is represented by gray bars.

small increase (11.5% average) in NQR subunits (Figure 7). *K. aerogenes* also seem to adapt its metabolism to utilize components present in host-like conditions (mAUM). SDH and the membrane-bound NADH-independent L-lactate dehydrogenase (LldD) showed a significant increase in expression and activity in mAUM (Figures 3, 7, respectively). SDH-dehydrogenase activity increased dramatically during growth in urine-like conditions and this correlates with an average fold-increase of SDH proteins of 1.5 (Figure 7). Citrate and α -ketoglutarate are molecules that enter the Krebs cycle which in turn increase the amount of succinate available for the SDH. Interestingly, a system involved in citrate uptake (Kästner et al., 2002; Scheu et al., 2012) was also upregulated, we found the sensor histidine kinase CitA (1.5 fold change ratio),

and the citrate-acetate antiporter CitW (3.4-fold change) content increased in mAUM compared to LB (Figure 7). Moreover, the α -ketoglutarate transporter KtgP was also upregulated in mAUM (1.2-fold increase) (Figure 7). We also found an increase in the expression of LldD (1.8 fold) and the lactate transporter LldP (2.1-fold), indicating higher use of lactate in mAUM compared to LB. However, we found no changes in another membrane-bound LDH (Dld). Furthermore, of the two membrane-bound malate dehydrogenases (MQO) coded in the genome, we observed a change of 0.6 for Mqo1 and no changes in the content of Mqo2 (Figure 7). However, differences in the activity of malate-dependent quinone-oxidoreductase were not observed during oximetry analysis (Figure 3). Finally, changes in the expression of terminal

oxidases were analyzed. The activity of *bo*₃ and *bd*-I terminal oxidases was similar in both media employed. However, we found an average 1.5 fold-increase in expression of *bo*₃ in urine-like conditions (Figure 7). On the other hand, the expression of *CydA*, structural part of the *bd*-I complex, showed a small decrease (0.8 fold-change) while *CydC*, which is involved in the biogenesis of the *bd*-I enzyme, exhibited a 1.2 fold-increase (Figure 7). Altogether, proteomic and oximetric data suggests that *K. aerogenes* undergoes metabolic changes to adapt to growth in host-like fluids, utilizing the available substrates present.

Discussion

Opportunistic emerging pathogens are highly relevant in clinical settings due to their capacity to survive antibiotic treatment, which greatly complicates patient outcomes (Beckwith and Jahre, 1980; Petit et al., 1990; Chow, 1991; Diene et al., 2013; Wesevich et al., 2020). Among these pathogens, *K. aerogenes* has become increasingly problematic as it is resistant to first line antibiotics, and in some cases even to last resort drugs in pandrug-resistant strains (Tuon et al., 2015; Wesevich et al., 2020; Pan et al., 2021). Due to the number of antibiotic resistant infections, the CDC has ranked CRE, including several strains of *K. aerogenes*, as a priority for the development of new antibiotics (Centers for Disease Control and Prevention, 2019). Studying the metabolic adaptations of pathogenic bacteria is essential for the development of novel strategies to combat antibiotic resistance, as it highlights relevant enzymes that could be employed as drug targets. However, most studies are performed in conditions that are not relevant for the pathophysiology of the microorganism and do not simulate the host environment, potentially misleading the selection of targets. In fact, there are no studies that describe *K. aerogenes* metabolism in conditions that are relevant in the clinical setting. In this work, we carried out a systematic characterization of the *K. aerogenes* respiratory chain in standard laboratory conditions and in conditions that simulate a common site of infection, the urinary tract. Studying the growth and metabolism of *K. aerogenes* in mAUM, we obtained data from conditions that closely resemble the environment in the urine, which has led us to identify critical enzymes that could be used to produce the desperately needed novel antibiotics.

Growth dynamics in urinary media

Most research involving *K. aerogenes* is focused on fermentation using different carbon sources (Kucharska et al., 2019; Wu et al., 2021; Boonyawanich et al., 2023), with little to no information regarding clinically relevant conditions. In nature and during infection, bacteria are rarely in an environment with optimal conditions for growth, therefore results obtained in laboratory media, like LB broth, do not represent the behavior within the host. Thus, we decided to investigate the respiratory metabolism of *K. aerogenes* in media that mimics urine, in which the bacterium should have significant adaptations, as previous studies have shown that bacterial pathogens carry specific sets of genes for the adaptation of bacteria to these environments (Frick-Cheng et al., 2020; Liang et al., 2020).

Klebsiella aerogenes showed a typical growth curve in both LB media and in mAUM. While *K. aerogenes* biomass and growth rate

are lower compared to LB media, this organism can still grow significantly in mAUM. Urine-like conditions impose a metabolic and physical burden due to high salinity, low pH, and low nutrient content and composition. However, *K. aerogenes* can still grow in these conditions, suggesting that this pathogen can replicate efficiently during urinary tract infections. Our results also show that *K. aerogenes* may reach stationary phase relatively fast during growth in urine-like conditions. This becomes relevant as tolerance to antibiotics develops during this phase, when bacterial growth rate and metabolism are markedly reduced (Brauner et al., 2016), which could be another factor that contributes to the intrinsic resistance of *K. aerogenes* to antibiotics.

Klebsiella aerogenes respiratory adaptations in urine-like conditions

mAUM, a medium recently developed by our group that closely resembles the composition of human urine, is more stable and reliable compared to other AUM (Brooks and Keevil, 1997; Liang et al., 2020). Moreover, we have previously shown that it supports the growth of *P. aeruginosa*, a common pathogen of the urinary tract and catheter-associated urinary tract infections (Rossolini and Mantengoli, 2005; Mittal et al., 2009; Liang et al., 2020; Ronald, 2002). mAUM is a relatively nutrient-poor medium that, as shown here, can also support the growth of *K. aerogenes*, which switches its metabolism in order to survive in this environment by significantly activating succinate and lactate dehydrogenases. Urine-like mAUM contains physiological amounts of L-lactate (Kramer et al., 1972) and citrate (Wein et al., 2011), thus the activation of membrane-bound lactate dehydrogenases and the Krebs cycle is expected. Interestingly, other pathogenic bacteria do not use the same metabolic strategies found here (Liang et al., 2020). For instance, our group has previously studied *P. aeruginosa* under similar conditions and we have found that SDH and LDH activities were not increased in mAUM (Liang et al., 2020), highlighting the importance of studying each pathogen independently.

Bd oxidase as the main terminal oxidase in *Klebsiella aerogenes*

Bioinformatics analysis showed that *K. aerogenes* carries one *cyoABCDE* operon and four *bd*-type terminal oxidase operons, two for type I *bd* and two for type II *bd* enzymes, making this the highest number of *bd*-type oxidases reported, with most microorganisms carrying only one operon (Forte et al., 2017). Our results show that *bd*-oxidases carry out 76–81% of the respiratory activity in *K. aerogenes*, a different metabolic strategy compared to other microorganisms. In other bacteria, *bo*₃ enzymes are the terminal oxidases preferentially used in oxygen-rich environments (Tseng et al., 1996). Indeed, we have reported that in *P. aeruginosa*, which carries the three types of terminal oxidases described above, *bo*₃ oxidase acts as the main terminal oxidase (Liang et al., 2020), resembling the case of *E. coli* and *Gluconobacter*, where *bo*₃ oxidase has also been reported as the main oxidase (Tseng et al., 1996; Richhardt et al., 2013). Thus, our results show that the metabolic strategies used by *K. aerogenes* are different compared to those of other pathogens.

Our proteomic results show that the *bd*-I oxidase is used by *K. aerogenes* during logarithmic growth. However, *bd*-II enzymes may be employed by *K. aerogenes* in other environmental conditions, providing a wide repertoire that allows adaptation to different environments. While the role of terminal oxidases in pathogenesis remains unclear, it has been proposed that *bd*-I oxidases are expressed in conditions where oxygen tension is below 50% (Grund et al., 2021). Additionally, it has been reported that *bd*-type enzymes act as ROS scavengers. Indeed, in *E. coli*, *bd*-type enzymes have peroxidase-like and catalase-like activities (Borisov et al., 2011a; Lu et al., 2015; Al-Attar et al., 2016; Forte et al., 2017; Borisov et al., 2021), which could be a mechanism of defense against the immune system and a factor that might determine pathogenicity. Our data indicate that *K. aerogenes* uses cytochrome *bd*-I oxidase encoded by the operon *cydABX-1* as the main terminal oxidase. *Bd*-I oxidases could be important for *K. aerogenes* as they might contribute to the rapid growth and colonization of human tissues during infection. In *Salmonella*, *bd*-I oxidases appear to provide a fitness advantage during the colonization of mouse tissues (Rivera-Chávez et al., 2016). On the other hand, in *E. coli*, *bd*-II oxidases are expressed upon entry to stationary phase and by phosphate starvation (Brøndsted and Atlung, 1996; Grund et al., 2021), suggesting that these enzymes could be more relevant during the switch to anaerobic growth (Brøndsted and Atlung, 1996; Tseng et al., 1996; Grund et al., 2021). *Bd*-II type oxidases have also been linked to fitness advantages following antibiotic treatment in mice (Rivera-Chávez et al., 2016).

Our results also show that *K. aerogenes* terminal oxidases have different sensitivities to cyanide compared to other enzymes of the same family. In most instances, *bd* oxidases tolerate high cyanide concentrations. For example, in *P. aeruginosa* the cyanide concentration needed to reach 50% inhibition (IC_{50}) ranges from 3 to 30 mM, depending on growth conditions (Matsushita et al., 1983; Forte et al., 2017). For *E. coli*, a concentration of 2 mM is required to observe the same effect (Forte et al., 2017; Liang et al., 2020). However, these values are highly variable and there are instances where *bd* oxidases are not severely tolerant to cyanide. For instance, the *bd* oxidases of *Photobacterium phosphoreum* and *Geobacillus thermodenitrificans* have IC_{50} of 62 μ M and 500 μ M, respectively (Konishi et al., 1986; Sakamoto et al., 1999), within the range that we are reporting for *K. aerogenes*, 150 μ M. These results suggest that *K. aerogenes* *bd*-type enzymes carry differences in structure that make them more susceptible to inhibition by KCN compared to other enzymes. Interestingly, *bd*-type enzymes are only present in prokaryotic organisms and are associated with colonization of host tissue (Rivera-Chávez et al., 2016), making them an attractive target for drug development (Forte et al., 2017). Their differences in KCN sensitivity may suggest that they could be differentially inhibited by newly designed drugs without affecting *bd*-type enzymes from the host microbiota, offering an important advantage compared to traditional antibiotics.

NDH-2 is the main NADH dehydrogenase in *Klebsiella aerogenes*

In this work, we are describing that *K. aerogenes* NDH-2 likely forms homodimers, as has been reported in other cases (Heikal et al.,

2014). Interestingly, in other organisms NDH-2 can also form supercomplexes with other respiratory enzymes, such as lactate dehydrogenases and ATPase subunits (Grandier-Vazeille et al., 2001). Moreover, proteomic analysis demonstrates that *K. aerogenes* employs a D₂ class NDH-2, which is different compared to *M. tuberculosis* D4 and *S. aureus* D1 classes (Marreiros et al., 2016). Our group and others have demonstrated that NQR is the main NADH dehydrogenase in many pathogenic microorganisms such as *P. aeruginosa* (Liang et al., 2020), *Vibrio cholerae* (Tuz et al., 2015; Agarwal et al., 2020), *C. trachomatis* (Liang et al., 2018), *Bacteroides fragilis* (Ito et al., 2020) and *Prevotella* spp. (Deusch et al., 2019), maintaining the motive force across the membrane and providing energy for ATP production and other vital processes. However, *K. aerogenes* does not seem to fit within this seemingly emerging trend in pathogens. We found that in *K. aerogenes*, NDH-2 is the main entry of electrons into the respiratory chain in the conditions tested, which represent widely different environments, while NDH-1 and NQR contribute to a small fraction of NADH-dehydrogenase activity. Previous works have shown that deletion of the NDH-1 genes *nuoD* and *nuoC* do not impact *K. aerogenes* growth (Wu et al., 2021), corroborating the data found here. In addition to *K. aerogenes*, other pathogens also rely heavily on NDH-2 in their respiratory metabolism, especially in those where NQR is absent (Schurig-Briccio et al., 2014; Lencina et al., 2018; Beites et al., 2019). For instance, in *Streptococcus agalactiae* the elimination of NDH-2 heavily impacts its capacity to colonize mouse kidney (Lencina et al., 2018). NDH-2 is a key enzyme during growth in enriched or in nutrient-limited conditions, suggesting that its loss or inhibition may critically impair *K. aerogenes* growth, causing cell death or allowing other drugs to exert their effects more efficiently, which opens opportunities to identify and design new drugs that target this enzyme against extensively drug-resistant or pan-resistant *K. aerogenes* strains.

Klebsiella aerogenes metabolism in urine-like media

Klebsiella aerogenes is a common constituent of the normal human microbiota and in certain conditions, it can become a facultative pathogen, producing one of the most common types of multidrug resistant UTIs (Lodise et al., 2022). In this work, we have elucidated for the first time the metabolic adaptations of this pathogen for the growth in urine-like media and likely during UTIs. *K. aerogenes* is able to employ the components present in mAUM, particularly citrate and lactate, to grow in this nutrient-poor environment. Our data analysis shows that SDH and LDH dehydrogenases, as well as citrate metabolism are activated in urine-like conditions. Moreover, we also observed an increase in the content of CitA, part of a two-component system involved in citrate transport, and the citrate-acetate antiporter CitW. Additionally, the expression of the α -ketoglutarate transporter KgtP was also found increased in these conditions. In a similar manner, the LldD lactate dehydrogenase and its related transporter, LldP, were increased in substantial amounts in mAUM, suggesting that lactate is being employed as a metabolite and the enzymatic machinery to transport it and oxidize is being upregulated. Overall, the content of enzymes that carry important roles in the Krebs cycle

was increased as an adaptation for the bacteria to growth in urine-like conditions to utilize the substrates present in these conditions.

While the composition of urine varies between individuals, an average composition has been previously reported (Kramer et al., 1972), showing significant amounts of citrate and lactate, at concentrations close to our urine-like formulation (Kramer et al., 1972). Our results suggest that *K. aerogenes* is able to metabolize citrate through the Krebs cycle, which produces succinate, while also being able to use lactate as source of electrons.

Our data show that at least three transporters that mobilize substrates for the Krebs cycle, KtgP, LldP and CitW, have increased expression in cells grown in mAUM. It has been demonstrated that KtgP and LldP are symporters that require protons to translocate their molecular targets (Seol and Shatkin, 1992; Núñez et al., 2002), therefore, a PMF gradient is required for their activity (Zhang et al., 2015). In urine-like media, while NDH-2 functions as the main dehydrogenase in the conditions studied, its activity is unable to contribute to the PMF gradient for these transporters or other processes since it is a non-proton pumping enzyme (Vamshi Krishna and Venkata Mohan, 2019). However, there is an increase in NDH-1 expression in urine-like media, which is able to pump 4 protons into the outer face of the membrane per electron pair (Bekker et al., 2009; Sazanov, 2015), explaining why *K. aerogenes* increases the expression of this dehydrogenase.

We found that the activity of *bd-I* is higher compared to the activity of *bo₃*, even though the last one pumps more protons per electron (*bo₃*: H⁺/e⁻ = 2; *bd-I*: H⁺/e⁻ = 1) (Bekker et al., 2009; Borisov et al., 2011b). Interestingly, *K. aerogenes* respiratory chain, composed mainly of NDH-2, SDH and *bd-I* oxidase would appear to pump only two protons per electron pair. Therefore, the respiratory chain that we are reporting is peculiar because the number of protons pumped per electron is limited, making it seemingly inefficient. However, there might be physiological adaptations for this, such as energy expenditure for protein production where the smaller *bd-I* might be preferred, an interest research avenue in the future.

Finally, according to the proteomic data, the expression of the *bo₃* terminal oxidases was also significantly increased in mAUM compared to LB, but their activity in both conditions remains the same, which may suggest that these enzymes are starting to be upregulated at this point. On the other hand, *bd-I* structural proteins had a reduced expression, but their biogenesis proteins had a significant fold-increase, which would be an important point of further examination to understand *K. aerogenes* metabolic adaptations. Consequently, our results point toward a metabolic shift in *K. aerogenes* to survive in the nutrient-poor environment of mAUM. This media simulates the human urine, and we demonstrate that this pathogen is well equipped to quickly and efficiently employ the components of this cell-free human-like fluid alone to grow to the stationary phase.

Concluding remarks

The data presented here describe the respiratory chain of *K. aerogenes*, an opportunistic pathogen of great clinical relevance. We found that the respiratory metabolism of this bacterium

differs from other gram-negative species, *K. aerogenes* preferentially uses NDH-2 dehydrogenases to pump electrons into the electron transport chain while also employing SDH and LDH enzymes during growth in urine-like conditions. As shown here, most of the respiratory activity is carried out by a *bd-I* oxidase. However, this bacterium encodes several *bd*-type oxidases, the highest reported to date in a single microorganism, with previously unknown roles. These data are critically important for the development of new drugs which target respiratory metabolism, as bacterial NDH-2 dehydrogenases and *bd-I* oxidoreductases are not present in human cells.

Data availability statement

The original contributions presented in the study are included in the article/Supplementary material, further inquiries can be directed to the corresponding author.

Ethics statement

Ethical approval was not required for the studies on humans in accordance with the local legislation and institutional requirements because only commercially available established cell lines were used.

Author contributions

MG-M: Data curation, Formal analysis, Investigation, Methodology, Validation, Visualization, Writing – original draft, Writing – review & editing. JS: Data curation, Formal analysis, Investigation, Writing – review & editing. GB: Investigation, Writing – original draft. OJ: Data curation, Formal analysis, Funding acquisition, Methodology, Resources, Validation, Writing – original draft, Writing – review & editing. KT: Conceptualization, Data curation, Formal analysis, Funding acquisition, Methodology, Project administration, Resources, Supervision, Validation, Writing – original draft, Writing – review & editing.

Funding

The author(s) declare financial support was received for the research, authorship, and/or publication of this article. This study was supported by grant R01 NIAID – 1R01AI151152 (OJ and KT). The content is solely the responsibility of the authors and does not necessarily represent the official views of the National Institutes of Health.

Acknowledgments

The authors would like to acknowledge the NIH s10 shared instrumentation grant (1S10OD027016-01) for supporting the work performed at the proteomics center at UIC.

Conflict of interest

The authors declare that the research was conducted in the absence of any commercial or financial relationships that could be construed as a potential conflict of interest.

Publisher's note

All claims expressed in this article are solely those of the authors and do not necessarily represent those of their affiliated

organizations, or those of the publisher, the editors and the reviewers. Any product that may be evaluated in this article, or claim that may be made by its manufacturer, is not guaranteed or endorsed by the publisher.

Supplementary material

The Supplementary material for this article can be found online at: <https://www.frontiersin.org/articles/10.3389/fmicb.2024.1479714/full#supplementary-material>

References

- Agarwal, S., Bernt, M., Toulouse, C., Kurz, H., Pfannstiel, J., D'Alvise, P., et al. (2020). Impact of Na⁺-translocating NADH: Quinone oxidoreductase on Iron uptake and *nqrM* expression in *Vibrio cholerae*. *J. Bacteriol.* 202:e00681-19. doi: 10.1128/JB.00681-19
- Al-Attar, S., Yu, Y., Pinkse, M., Hoese, J., Friedrich, T., Bald, D., et al. (2016). Cytochrome *bd* displays significant Quinol peroxidase activity. *Sci. Rep.* 6:27631. doi: 10.1038/srep27631
- Allerberger, F., Koeuth, T., Lass-Flörl, C., Dierich, M. P., Putensen, C., Schmutzhard, E., et al. (1996). Epidemiology of infection due to multidrug-resistant *Enterobacter aerogenes* in a university hospital. *Eur. J. Clin. Microbiol. Infect. Dis.* 15, 517–521. doi: 10.1007/BF01691323
- Arpin, C., Coze, C., Rogues, A. M., Gachie, J. P., Bebear, C., and Quentin, C. (1996). Epidemiological study of an outbreak due to multidrug-resistant *Enterobacter aerogenes* in a medical intensive care unit. *J. Clin. Microbiol.* 34, 2163–2169. doi: 10.1128/jcm.34.9.2163-2169.1996
- Arpin, C., Dubois, V., Coulangue, L., André, C., Fischer, I., Noury, P., et al. (2003). Extended-Spectrum β -lactamase-producing *Enterobacteriaceae* in community and private health care centers. *Antimicrob. Agents Chemother.* 47, 3506–3514. doi: 10.1128/AAC.47.11.3506-3514.2003
- Arpin, C., Dubois, V., Maugein, J., Jullin, J., Dutilh, B., Brochet, J.-P., et al. (2005). Clinical and molecular analysis of extended-Spectrum β -lactamase-producing *Enterobacteria* in the community setting. *J. Clin. Microbiol.* 43, 5048–5054. doi: 10.1128/JCM.43.10.5048-5054.2005
- Barquera, B., Hellwig, P., Zhou, W., Morgan, J. E., Häse, C. C., Gosink, K. K., et al. (2002). Purification and characterization of the recombinant Na⁺-translocating NADH:Quinone oxidoreductase from *Vibrio cholerae*. *Biochemistry* 41, 3781–3789. doi: 10.1021/bi011873o
- Beckwith, D. G., and Jahre, J. A. (1980). Role of a cefoxitin-inducible beta-lactamase in a case of breakthrough bacteremia. *J. Clin. Microbiol.* 12, 517–520. doi: 10.1128/jcm.12.4.517-520.1980
- Beites, T., O'Brien, K., Tiwari, D., Engelhart, C. A., Walters, S., Andrews, J., et al. (2019). Plasticity of the *Mycobacterium tuberculosis* respiratory chain and its impact on tuberculosis drug development. *Nat. Commun.* 10:4970. doi: 10.1038/s41467-019-12956-2
- Bekker, M., De Vries, S., Ter Beek, A., Hellingwerf, K. J., and De Mattos, M. J. T. (2009). Respiration of *Escherichia coli* can be fully uncoupled via the non-electrogenic terminal cytochrome *bd*-II oxidase. *J. Bacteriol.* 191, 5510–5517. doi: 10.1128/JB.00562-09
- Bogachev, A. V., Murtazina, R. A., and Skulachev, V. P. (1997). The Na⁺/e⁻ stoichiometry of the Na⁺-motive NADH: quinone oxidoreductase in *Vibrio alginolyticus*. *FEBS Lett.* 409, 475–477. doi: 10.1016/S0014-5793(97)00536-X
- Boonyawanich, S., Haosagul, S., and Pisutpaisal, N. (2023). Ethanol production from waste glycerol using glucose as co-carbon source. *Biomass Convers. Biorefinery* 13, 2769–2778. doi: 10.1007/s13399-021-01325-z
- Borisov, V. B., Gennis, R. B., Hemp, J., and Verkhovskiy, M. I. (2011a). The cytochrome *bd* respiratory oxygen reductases. *Biochim. Biophys. Acta* 1807, 1398–1413. doi: 10.1016/j.bbabi.2011.06.016
- Borisov, V. B., Murali, R., Verkhovskaya, M. L., Bloch, D. A., Han, H., Gennis, R. B., et al. (2011b). Aerobic respiratory chain of *Escherichia coli* is not allowed to work in fully uncoupled mode. *Proc. Natl. Acad. Sci.* 108, 17320–17324. doi: 10.1073/pnas.1108217108
- Borisov, V. B., Siletsky, S. A., Nastasi, M. R., and Forte, E. (2021). ROS defense systems and terminal oxidases in Bacteria. *Antioxidants* 10:839. doi: 10.3390/antiox10060839
- Brandt, U. (2006). Energy converting NADH: Quinone oxidoreductase (complex I). *Annu. Rev. Biochem.* 75, 69–92. doi: 10.1146/annurev.biochem.75.103004.142539
- Brauner, A., Fridman, O., Gefen, O., and Balaban, N. Q. (2016). Distinguishing between resistance, tolerance and persistence to antibiotic treatment. *Nat. Rev. Microbiol.* 14, 320–330. doi: 10.1038/nrmicro.2016.34
- Brøndsted, L., and Atlung, T. (1996). Effect of growth conditions on expression of the acid phosphatase (*cyx-appA*) operon and the *appY* gene, which encodes a transcriptional activator of *Escherichia coli*. *J. Bacteriol.* 178, 1556–1564. doi: 10.1128/jb.178.6.1556-1564.1996
- Brooks, T., and Keevil, C. W. (1997). A simple artificial urine for the growth of urinary pathogens. *Lett. Appl. Microbiol.* 24, 203–206. doi: 10.1046/j.1472-765X.1997.00378.x
- Centers for Disease Control and Prevention (2019). Antibiotic resistance threats in the United States, 2019. Atlanta, GA: Centers for Disease Control and Prevention.
- Chow, J. W. (1991). *Enterobacter* bacteremia: clinical features and emergence of antibiotic resistance during therapy. *Ann. Intern. Med.* 115, 585–590. doi: 10.7326/0003-4819-115-8-585
- D'Alessandro, M., Erb, M., Ton, J., Brandenburg, A., Karlen, D., Zopfi, J., et al. (2014). Volatiles produced by soil-borne endophytic bacteria increase plant pathogen resistance and affect tritrophic interactions: bacterial volatiles and multitrophic interactions. *Plant Cell Environ.* 37, 813–826. doi: 10.1111/pce.12220
- Davin-Regli, A., Monnet, D., Saux, P., Bosi, C., Charrel, R., Barthelemy, A., et al. (1996). Molecular epidemiology of *Enterobacter aerogenes* acquisition: one-year prospective study in two intensive care units. *J. Clin. Microbiol.* 34, 1474–1480. doi: 10.1128/jcm.34.6.1474-1480.1996
- Davin-Regli, A., and Pagés, J.-M. (2015). *Enterobacter aerogenes* and *Enterobacter cloacae*: versatile bacterial pathogens confronting antibiotic treatment. *Front. Microbiol.* 6:392. doi: 10.3389/fmicb.2015.00392
- Deusch, S., Bok, E., Schleicher, L., Seifert, J., and Steuber, J. (2019). Occurrence and function of the Na⁽⁺⁾-translocating NADH:Quinone oxidoreductase in *Prevotella* spp. *Microorganisms* 7:117. doi: 10.3390/microorganisms7050117
- Diene, S. M., Merhej, V., Henry, M., El Filali, A., Roux, V., Robert, C., et al. (2013). The rhizome of the multidrug-resistant *Enterobacter aerogenes* genome reveals how new "killer bugs" are created because of a sympatric lifestyle. *Mol. Biol. Evol.* 30, 369–383. doi: 10.1093/molbev/mss236
- Feng, Y., Li, W., Li, J., Wang, J., Ge, J., Xu, D., et al. (2012). Structural insight into the type-II mitochondrial NADH dehydrogenases. *Nature* 491, 478–482. doi: 10.1038/nature11541
- Forte, E., Borisov, V. B., Vicente, J. B., and Giuffrè, A. (2017). Cytochrome *bd* and gaseous ligands in bacterial physiology. *Adv. Microb. Physiol.* 71, 171–234. doi: 10.1016/bs.ampbs.2017.05.002
- Founou, R. C., Founou, L. L., and Essack, S. Y. (2017). Clinical and economic impact of antibiotic resistance in developing countries: a systematic review and meta-analysis. *PLoS One* 12:e0189621. doi: 10.1371/journal.pone.0189621
- Frick-Cheng, A. E., Sintsova, A., Smith, S. N., Krauthammer, M., Eaton, K. A., and Mobley, H. L. T. (2020). The gene expression profile of Uropathogenic *Escherichia coli* in women with uncomplicated urinary tract infections is recapitulated in the mouse model. *mBio* 11, e01412–e01420. doi: 10.1128/mBio.01412-20
- Gashe, F., Mulisa, E., Mekonnen, M., and Zeleke, G. (2018). Antimicrobial resistance profile of different clinical isolates against third-generation Cephalosporins. *J. Pharm.* 2018, 1–7. doi: 10.1155/2018/5070742
- Grandier-Vazeille, X., Bathany, K., Chaignepain, S., Camougrand, N., Manon, S., and Schmitter, J.-M. (2001). Yeast mitochondrial dehydrogenases are associated in a supramolecular complex. *Biochemistry* 40, 9758–9769. doi: 10.1021/bi010277r
- Grimont, P. A., and Grimont, F. (2005). "Genus XVI. *Klebsiella*" in Bergey's manual of systematic bacteriology. ed. G. M. Garrity (New York: Springer), 685–693.
- Grund, T. N., Radloff, M., Wu, D., Goojani, H. G., Witte, L. F., Jösting, W., et al. (2021). Mechanistic and structural diversity between cytochrome *bd* isoforms of *Escherichia coli*. *Proc. Natl. Acad. Sci.* 118:e2114013118. doi: 10.1073/pnas.2114013118
- Heikal, A., Nakatani, Y., Dunn, E., Weimar, M. R., Day, C. L., Baker, E. N., et al. (2014). Structure of the bacterial type II NADH dehydrogenase: a monotopic membrane protein

- with an essential role in energy generation: structure of bacterial NDH-2. *Mol. Microbiol.* 91, 950–964. doi: 10.1111/mmi.12507
- Hreha, T. N., Foreman, S., Duran-Pinedo, A., Morris, A. R., Diaz-Rodriguez, P., Jones, J. A., et al. (2021). The three NADH dehydrogenases of *Pseudomonas aeruginosa*: their roles in energy metabolism and links to virulence. *PLoS One* 16:e0244142. doi: 10.1371/journal.pone.0244142
- Itó, T., Gallegos, R., Matano, L. M., Butler, N. L., Hantman, N., Kaili, M., et al. (2020). Genetic and biochemical analysis of anaerobic respiration in *Bacteroides fragilis* and its importance *in vivo*. *mBio* 11, e03238–e03219. doi: 10.1128/mBio.03238-19
- Juárez, O., and Barquera, B. (2012). Insights into the mechanism of electron transfer and sodium translocation of the Na⁺-pumping NADH:quinone oxidoreductase. *Biochim. Biophys. Acta* 1817, 1823–1832. doi: 10.1016/j.bbabi.2012.03.017
- Juárez, O., Nilges, M. J., Gillespie, P., Cotton, J., and Barquera, B. (2008). Riboflavin is an active redox cofactor in the Na⁺-pumping NADH:quinone oxidoreductase (Na⁺-NQR) from *Vibrio cholerae*. *J. Biol. Chem.* 283, 33162–33167. doi: 10.1074/jbc.M806913200
- Karlsson, M., Lutgring, J. D., Ansari, U., Lawsin, A., Albrecht, V., McAllister, G., et al. (2022). Molecular characterization of Carbapenem-resistant *Enterobacterales* collected in the United States. *Microb. Drug Resist.* 28, 389–397. doi: 10.1089/mdr.2021.0106
- Kästner, C. N., Schneider, K., Dimroth, P., and Pos, K. M. (2002). Characterization of the citrate/acetate antiporter CitW of *Klebsiella pneumoniae*. *Arch. Microbiol.* 177, 500–506. doi: 10.1007/s00203-002-0420-8
- Knook, D. L., and Planta, R. J. (1971). Function of ubiquinone in Electron transport from reduced nicotinamide adenine dinucleotide to nitrate and oxygen in *Aerobacter aerogenes*. *J. Bacteriol.* 105, 483–488. doi: 10.1128/jb.105.2.483-488.1971
- Knook, D. L., and Planta, R. J. (1973). The function of ubiquinone in *Klebsiella aerogenes*. *Arch. Microbiol.* 93, 13–22. doi: 10.1007/BF00666077
- Konishi, K., Ouchi, M., Kita, K., and Horikoshi, I. (1986). Purification and properties of a Cytochrome b₅₆₀-d complex, a terminal oxidase of the aerobic respiratory chain of *Photobacterium phosphoreum*. *J. Biochem.* 99, 1227–1236. doi: 10.1093/oxfordjournals.jbchem.a135586
- Kramer, H. J., Lu, E., and Gonick, H. C. (1972). Organic acid excretion patterns in gout. *Ann. Rheum. Dis.* 31, 137–144. doi: 10.1136/ard.31.2.137
- Kucharska, K., Cieśliński, H., Rybarczyk, P., Ślupek, E., Łukajtis, R., Wychodnik, K., et al. (2019). Fermentative conversion of two-step pre-treated lignocellulosic biomass to hydrogen. *Catalysts* 9:858. doi: 10.3390/catal9100858
- Lencina, A. M., Franza, T., Sullivan, M. J., Ulett, G. C., Ipe, D. S., Gaudy, P., et al. (2018). Type 2 NADH dehydrogenase is the only point of entry for electrons into the *Streptococcus agalactiae* respiratory chain and is a potential drug target. *MBio* 9, e01034–e01018. doi: 10.1128/mBio.01034-18
- Liang, P., Fang, X., Hu, Y., Yuan, M., Raba, D. A., Ding, J., et al. (2020). The aerobic respiratory chain of *Pseudomonas aeruginosa* cultured in artificial urine media: role of NQR and terminal oxidases. *PLoS One* 15:e0231965. doi: 10.1371/journal.pone.0231965
- Liang, P., Rosas-Lemus, M., Patel, D., Fang, X., Tuz, K., and Juárez, O. (2018). Dynamic energy dependency of *Chlamydia trachomatis* on host cell metabolism during intracellular growth: role of sodium-based energetics in chlamydial ATP generation. *J. Biol. Chem.* 293, 510–522. doi: 10.1074/jbc.M117.797209
- Lodise, T. P., Chopra, T., Nathanson, B. H., Sulham, K., and Rodriguez, M. (2022). Epidemiology of complicated urinary tract infections due to *Enterobacterales* among adult patients presenting in emergency departments across the United States. *Open Forum Infect. Dis.* 9:ofac315. doi: 10.1093/ofid/ofac315
- Lu, P., Heineke, M. H., Koul, A., Andries, K., Cook, G. M., Lill, H., et al. (2015). The cytochrome *bd*-type quinol oxidase is important for survival of *Mycobacterium smegmatis* under peroxide and antibiotic-induced stress. *Sci. Rep.* 5:10333. doi: 10.1038/srep10333
- Mann, A., Malik, S., Rana, J. S., and Nehra, K. (2021). Whole genome sequencing data of *Klebsiella aerogenes* isolated from agricultural soil of Haryana, India. *Data Brief* 38:107311. doi: 10.1016/j.dib.2021.107311
- Marreiros, B. C., Sena, F. V., Sousa, F. M., Batista, A. P., and Pereira, M. M. (2016). Type II NADH:quinone oxidoreductase family: phylogenetic distribution, structural diversity and evolutionary divergences. *Environ. Microbiol.* 18, 4697–4709. doi: 10.1111/1462-2920.13352
- Matsushita, K., Yamada, M., Shinagawa, E., Adachi, O., and Ameyama, M. (1983). Membrane-bound respiratory chain of *Pseudomonas aeruginosa* grown aerobically. A KCN-insensitive alternate oxidase chain and its energetics. *J. Biochem.* 93, 1137–1144. doi: 10.1093/oxfordjournals.jbchem.a134239
- Melin, F., Meyer, T., Lankiang, S., Choi, S. K., Gennis, R. B., Blanck, C., et al. (2013). Direct electrochemistry of cytochrome *bo₃* oxidase at a series of gold nanoparticles-modified electrodes. *Electrochem. Commun.* 26, 105–108. doi: 10.1016/j.elecom.2012.10.024
- Melo, A. M. P., Bandejas, T. M., and Teixeira, M. (2004). New insights into type II NAD(P)H:quinone oxidoreductases. *Microbiol. Mol. Biol. Rev.* 68, 603–616. doi: 10.1128/MMBR.68.4.603-616.2004
- Meyers, H. B., Fontanilla, E., and Mascola, L. (1988). Risk factors for development of sepsis in a hospital outbreak of *Enterobacter aerogenes*. *Am. J. Infect. Control* 16, 118–122. doi: 10.1016/0196-6553(88)90050-8
- Mittal, R., Aggarwal, S., Sharma, S., Chhibber, S., and Harjai, K. (2009). Urinary tract infections caused by *Pseudomonas aeruginosa*: a minireview. *J. Infect. Public Health* 2, 101–111. doi: 10.1016/j.jiph.2009.08.003
- Mogi, T., Ano, Y., Nakatsuka, T., Toyama, H., Muroi, A., Miyoshi, H., et al. (2009). Biochemical and spectroscopic properties of cyanide-insensitive Quinol oxidase from *Gluconobacter oxydans*. *J. Biochem.* 146, 263–271. doi: 10.1093/jb/mvp067
- Mulani, M. S., Kamble, E. E., Kumkar, S. N., Tawre, M. S., and Pardesi, K. R. (2019). Emerging strategies to combat ESKAPE pathogens in the era of antimicrobial resistance: a review. *Front. Microbiol.* 10:539. doi: 10.3389/fmicb.2019.00539
- Muller, M. M., and Webster, R. E. (1997). Characterization of the *tol-pal* and *cyd* region of *Escherichia coli* K-12: transcript analysis and identification of two new proteins encoded by the *cyd* operon. *J. Bacteriol.* 179, 2077–2080. doi: 10.1128/jb.179.6.2077-2080.1997
- Nakatani, Y., Jiao, W., Aragão, D., Shimaki, Y., Petri, J., Parker, E. J., et al. (2017). Crystal structure of type II NADH:quinone oxidoreductase from *Caldalkalibacillus thermarum* with an improved resolution of 2.15 Å. *Acta Crystallogr. Acta Crystallogr. F Struct. Biol. Commun.* 73, 541–549. doi: 10.1107/S2053230X17013073
- Núñez, M. F., Kwon, O., Wilson, T. H., Aguilar, J., Baldoma, L., and Lin, E. C. C. (2002). Transport of L-lactate, D-lactate, and Glycolate by the LldP and GlcA membrane carriers of *Escherichia coli*. *Biochem. Biophys. Res. Commun.* 290, 824–829. doi: 10.1006/bbrc.2001.6255
- Pan, F., Xu, Q., and Zhang, H. (2021). Emergence of NDM-5 producing Carbapenem-resistant *Klebsiella aerogenes* in a pediatric Hospital in Shanghai, China. *Front. Public Health* 9:621527. doi: 10.3389/fpubh.2021.621527
- Petit, A., Gerbaud, G., Siro, D., Courvalin, P., and Siro, J. (1990). Molecular epidemiology of TEM-3 (CTX-1) β-lactamase. *Antimicrob. Agents Chemother.* 34, 219–224. doi: 10.1128/AAC.34.2.219
- Raba, D. A., Rosas-Lemus, M., Menzer, W. M., Li, C., Fang, X., Liang, P., et al. (2018). Characterization of the *Pseudomonas aeruginosa* NQR complex, a bacterial proton pump with roles in autopoisoning resistance. *J. Biol. Chem.* 293, 15664–15677. doi: 10.1074/jbc.RA118.003194
- Reyes-Prieto, A., Barquera, B., and Juárez, O. (2014). Origin and evolution of the sodium-pumping NADH: ubiquinone oxidoreductase. *PLoS One* 9:e96696. doi: 10.1371/journal.pone.0096696
- Richhardt, J., Luchterhand, B., Bringer, S., Buchs, J., and Bott, M. (2013). Evidence for a key role of cytochrome *bo₃* oxidase in respiratory energy metabolism of *Gluconobacter oxydans*. *J. Bacteriol.* 195, 4210–4220. doi: 10.1128/JB.00470-13
- Rivera-Chávez, F., Zhang, L. F., Faber, F., Lopez, C. A., Byndloss, M. X., Olsan, E. E., et al. (2016). Depletion of butyrate-producing Clostridia from the gut microbiota drives an aerobic luminal expansion of *Salmonella*. *Cell Host Microbe* 19, 443–454. doi: 10.1016/j.chom.2016.03.004
- Ronald, A. (2002). The etiology of urinary tract infection: Traditional and emerging pathogens. *Am. J. Med.* 113, 14S–19S. doi: 10.1016/s0002-9343(02)01055-0
- Rossolini, G. M., and Mantengoli, E. (2005). Treatment and control of severe infections caused by multiresistant *Pseudomonas aeruginosa*. *Clin. Microbiol. Infect.* 11, 17–32. doi: 10.1111/j.1469-0691.2005.01161.x
- Sakamoto, J., Koga, E., Mizuta, T., Sato, C., Noguchi, S., and Sone, N. (1999). Gene structure and quinol oxidase activity of a cytochrome *bd*-type oxidase from *Bacillus stearothermophilus*. *Biochim. Biophys. Acta* 1411, 147–158. doi: 10.1016/S0005-2728(99)00012-2
- Sazanov, L. A. (2015). A giant molecular proton pump: structure and mechanism of respiratory complex I. *Nat. Rev. Mol. Cell Biol.* 16, 375–388. doi: 10.1038/nrm3997
- Scheu, P. D., Witan, J., Rauschmeier, M., Graf, S., Liao, Y.-F., Ebert-Jung, A., et al. (2012). CitA/CitB two-component system regulating citrate fermentation in *Escherichia coli* and its relation to the DcuS/DcuR system *in vivo*. *J. Bacteriol.* 194, 636–645. doi: 10.1128/JB.06345-11
- Schurig-Briccio, L. A., Yano, T., Rubin, H., and Gennis, R. B. (2014). Characterization of the type 2 NADH:menaquinone oxidoreductases from *Staphylococcus aureus* and the bactericidal action of phenothiazines. *Biochim. Biophys. Acta* 1837, 954–963. doi: 10.1016/j.bbabi.2014.03.017
- Seol, W., and Shatkin, A. J. (1992). *Escherichia coli* a-ketoglutarate permease is a constitutively expressed proton symporter. *J. Biol. Chem.* 267, 6409–6413. doi: 10.1016/S0021-9258(18)42710-X
- Souza Lopes, A. C., Rodrigues, J. F., Cabral, A. B., Da Silva, M. E., Leal, N. C., Da Silveira, V. M., et al. (2016). Occurrence and analysis of *irp2* virulence gene in isolates of *Klebsiella pneumoniae* and *Enterobacter* spp. from microbiota and hospital and community-acquired infections. *Microb. Pathog.* 96, 15–19. doi: 10.1016/j.micpath.2016.04.018
- Szczerba, H., Komoń-Janczara, E., Dudziak, K., Waśko, A., and Targoński, Z. (2020). A novel biocatalyst, *Enterobacter aerogenes* LU2, for efficient production of succinic acid using whey permeate as a cost-effective carbon source. *Biotechnol. Biofuels* 13:96. doi: 10.1186/s13068-020-01739-3
- Tseng, C. P., Albrecht, J., and Gunsalus, R. P. (1996). Effect of microaerophilic cell growth conditions on expression of the aerobic (*cyoABCDE* and *cydAB*) and anaerobic (*narGHJ*, *frdABCD*, and *dmsABC*) respiratory pathway genes in *Escherichia coli*. *J. Bacteriol.* 178, 1094–1098. doi: 10.1128/jb.178.4.1094-1098.1996
- Tuon, F. F., Scharf, C., Rocha, J. L., Cieslinski, J., Becker, G. N., and Arend, L. N. (2015). KPC-producing *Enterobacter aerogenes* infection. *Braz. J. Infect. Dis.* 19, 324–327. doi: 10.1016/j.bjid.2015.01.003
- Tuz, K., Mezic, K. G., Xu, T., Barquera, B., and Juárez, O. (2015). The kinetic reaction mechanism of the *Vibrio cholerae* sodium-dependent NADH dehydrogenase. *J. Biol. Chem.* 290, 20009–20021. doi: 10.1074/jbc.M115.658773
- Vamshi Krishna, K., and Venkata Mohan, S. (2019). Purification and characterization of NDH-2 protein and elucidating its role in extracellular Electron

- transport and Bioelectrogenic activity. *Front. Microbiol.* 10:880. doi: 10.3389/fmicb.2019.00880
- Wein, A. J., Kavoussi, L. R., Novick, A. C., and Peters, C. A. (2011). *Campbell-Walsh Urology*. Philadelphia: Elsevier.
- Weiss, S. A., Bushby, R. J., Evans, S. D., and Jeuken, L. J. C. (2010). A study of cytochrome *bo*₃ in a tethered bilayer lipid membrane. *Biochim. Biophys. Acta* 1797, 1917–1923. doi: 10.1016/j.bbabi.2010.01.012
- Wesevich, A., Sutton, G., Ruffin, F., Park, L. P., Fouts, D. E., Fowler, V. G., et al. (2020). Newly named *Klebsiella aerogenes* (formerly *Enterobacter aerogenes*) is associated with poor clinical outcomes relative to other *Enterobacter* species in patients with bloodstream infection. *J. Clin. Microbiol.* 58, e00582–e00520. doi: 10.1128/JCM.00582-20
- World Health Organization (2017). WHO publishes list of bacteria for which new antibiotics are urgently needed. Available at: <https://www.who.int/news/item/27-02-2017-who-publishes-list-of-bacteria-for-which-new-antibiotics-are-urgently-needed>.
- Wu, Y., Chu, W., Yang, J., Xu, Y., Shen, Q., Yang, H., et al. (2021). Metabolic engineering of *Enterobacter aerogenes* for improved 2,3-Butanediol production by manipulating NADH levels and overexpressing the small RNA RyhB. *Front. Microbiol.* 12:754306. doi: 10.3389/fmicb.2021.754306
- Yagi, T. (1991). Bacterial NADH-quinone oxidoreductases. *J. Bioenerg. Biomembr.* 23, 211–225. doi: 10.1007/BF00762218
- Yip, C., Harbour, M. E., Jayawardena, K., Fearnley, I. M., and Sazanov, L. A. (2011). Evolution of respiratory complex I. *J. Biol. Chem.* 286, 5023–5033. doi: 10.1074/jbc.M110.194993
- Zhang, X. C., Zhao, Y., Heng, J., and Jiang, D. (2015). Energy coupling mechanisms of MFS transporters. *Protein Sci.* 24, 1560–1579. doi: 10.1002/pro.2759
- Zhou, W., Bertsova, Y. V., Feng, B., Tsatsos, P., Verkhovskaya, M. L., Gennis, R. B., et al. (1999). Sequencing and preliminary characterization of the Na⁺-translocating NADH:ubiquinone oxidoreductase from *Vibrio harveyi*. *Biochemistry* 38, 16246–16252. doi: 10.1021/bi991664s
- Zickermann, V., Kurki, S., Kervinen, M., Hassinen, I., and Finel, M. (2000). The NADH oxidation domain of complex I: do bacterial and mitochondrial enzymes catalyze ferricyanide reduction similarly? *Biochim. Biophys. Acta* 1459, 61–68. doi: 10.1016/S0005-2728(00)00113-4